Nitric Oxide 87 (2019) 60–72

Contents lists available at ScienceDirect

Nitric Oxide

journal homepage: www.elsevier.com/locate/yniox

Altered neurovascular coupling and brain arginine metabolism in endothelial nitric oxide synthase deficient mice

Ashwini Hariharan[a], Yu Jing[a], Nicola D. Collie[a], Hu Zhang[b], Ping Liu[a,*]

[a] Department of Anatomy, School of Biomedical Sciences, Brain Health Research Centre, University of Otago, Brain Research New Zealand, New Zealand
[b] School of Pharmacy, Brain Health Research Centre, University of Otago, Brain Research New Zealand, New Zealand

ARTICLE INFO

Keywords:
eNOS deficiency
Cerebral blood flow
Neurovascular coupling
Nitric oxide
Arginine metabolism
Glutamine

ABSTRACT

Nitric oxide (NO) produced by endothelial NO synthase (eNOS) is a key regulator of cerebral blood flow (CBF) dynamics. Mice with eNOS deficiency ($eNOS^{-/-}$) display age-related increases in amyloid beta in the brain and memory deficits, implicating eNOS dysfunction in the neuropathogenesis and/or development of Alzheimer's disease (AD). The present study systematically investigated behavioural, CBF and brain arginine metabolic profile changes in male and female wildtype (WT) and $eNOS^{-/-}$ mice at 14 months of age. $eNOS^{-/-}$ mice displayed altered behaviour in the Y-maze and open field tests. A real-time microcirculation imager revealed a significant sex difference in the basal CBF and significantly increased perfusion response to whisker stimulations in the Barrel cortex in both male and female $eNOS^{-/-}$ mice relative to their sex-matched WT controls. The treatment of 7-nitroindazole blocked the increased perfusion response to whisker stimulations in $eNOS^{-/-}$ mice. Neurochemically, the most intriguing changes were markedly reduced glutamine levels in both male and female $eNOS^{-/-}$ mice in the frontal cortex, hippocampus, parahippocampal region and cerebellum. These findings demonstrate altered behavioural function, neurovascular coupling and brain arginine metabolism (glutamine in particular) under the condition of eNOS deficiency, which further supports the role of eNOS dysfunction in the AD neuropathogenesis.

1. Introduction

Alzheimer's disease (AD) is the most common cause of dementia in the aged. It is characterised by the neuropathological hallmarks of senile plaques (SPs) and neurofibrillary tangles (NFTs). The most commonly held view regarding the primary pathophysiological event in AD centres on the amyloid cascade hypothesis [1], which states that AD begins with the assembly and accumulation of amyloid beta (Aβ) derived from the amyloid-β precursor protein (APP). Although the amyloid hypothesis has dominated the AD field for over 20 years, every clinical trial for AD treatment targeting Aβ peptides and amyloids has failed [2]. A critical question regarding its causality has therefore been increasingly raised [3]. Recent evidence suggests that chronic cerebral hypoperfusion due to cerebrovascular endothelial dysfunction during advanced aging leads to an energy crisis that may trigger the neurodegenerative processes in AD [3–5]. In AD brains, there are reduced resting cerebral blood flow (CBF), vascular anatomical defects and impaired blood brain barrier function, which could contribute to the accumulation and faulty clearance of Aβ [6].

There is a growing body of evidence implicating altered metabolism of L-arginine in the pathogenesis of AD [4,7–11]. L-arginine is a semi-essential amino acid with a number of bioactive metabolites (Fig. 1) [12]. Nitric oxide (NO) is a gaseous signaling molecule produced by nitric oxide synthase (NOS) [13]. It has been well documented that NO derived from neuronal NOS (nNOS) plays an important role in neurotransmission, synaptic plasticity and learning and memory [14–16], whereas endothelial NOS (eNOS)-derived NO is a major regulator of CBF, hence a key player in the cerebrovascular dynamics [17]. Due to its nature as a free radical, however, an excessive amount of NO, particularly that derived from inducible NOS (iNOS), is neurotoxic and leads to neurodegeneration [7,18]. It has been shown that AD brains have reduced eNOS expression in cerebral vessels and virtually no eNOS expression in many small and medium-sized leptomeningeal, cortical, and white matter vessels [19]. Moreover, SPs and NFTs are associated with reduced capillary expression of eNOS [20,21]. Contrarily, Luth and colleagues found similar eNOS expression in endothelial cells and astrocytes of normal and AD brains, but increased immunoreactive intensity of eNOS-positive astrocytes that was associated with SPs in the AD cases [22,23]. We have recently determined AD- and age-related changes in eNOS protein expression in the

* Corresponding author. Dr. Ping Liu, Department of Anatomy, University of Otago, Dunedin, New Zealand.
E-mail address: ping.liu@otago.ac.nz (P. Liu).

https://doi.org/10.1016/j.niox.2019.03.006
Received 21 December 2018; Received in revised form 6 March 2019; Accepted 10 March 2019
Available online 13 March 2019

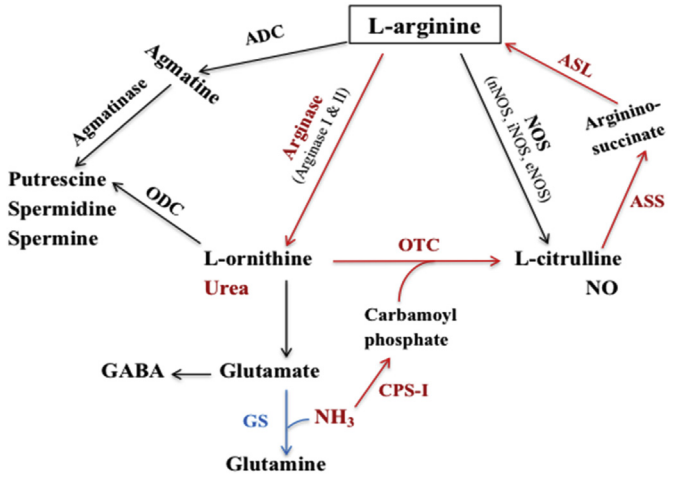

Fig. 1. L-arginine metabolic pathways. L-arginine is metabolized by nitric oxide synthase (NOS) to form L-citrulline and nitric oxide (NO), by arginase to produce L-ornithine and urea, and by arginine decarboxylase (ADC) to form agmatine. Ornithine decarboxylase (ODC) and agmatinase can metabolise L-ornithine and agmatine respectively to produce polyamines putrescine, spermidine and spermine. L-ornithine can also be channeled to form glutamate, glutamine and GABA. The urea cycle is comprised of carbamyl phosphate synthetase-I (CPS-I), ornithine transcarbamylase (OTC), argininosuccinate synthetase (ASS), argininosuccinate lyase (ASL) and arginase to dispose of toxic ammonia (NH3) in the non-toxic form of urea (indicated by red arrows). In normal adult brains, the urea cycle is incomplete (hence inactive) due to the lack of OTC. Under physiological conditions, brain ammonia is metabolized to glutamine by glutamine synthetase (GS). Abbreviations: eNOS, endothelial nitric oxide synthase; GABA, γ-aminobutyric acid; iNOS, inducible NOS; nNOS, neuronal NOS.

hippocampus and superior frontal gyrus, and found a dramatic (~95%) reduction in the AD cases relative to their age-matched control cases (mean age 80 years) and lesser (30–70%) reductions in the 80-year control group when compared to the 60-year control group [7]. These results demonstrate the presence of eNOS deficiency in AD and advanced aged brains, and suggest that such age-related eNOS deficiency may be an early event contributing to later neurodegeneration [8]. Intriguingly, research shows that eNOS-derived NO can directly modulate the production of Aβ and protect against increases in Aβ [24,25]. Mice with eNOS deficiency ($eNOS^{-/-}$) display behavioural changes and memory deficits, altered neuronal p25 (an aberrant activator of the tau kinase Cdk5), and increased levels of APP, β-site APP cleaving enzyme 1 (BACE1) and Aβ in the brain [26,27]. These findings suggest that loss of eNOS-derived NO contributes to amyloidogenic processing of APP, tau phosphorylation and cognitive decline.

The neurovascular unit is a tight network comprising of endothelial cells, pericytes, smooth muscle cells, glia and neurons, and governs the coupling of neuronal activity with changes in regional CBF (i.e., neurovascular coupling) [28,29]. Altered neurovascular coupling is prominent in AD, and could be due to decreased demand by the tissue or inadequacy of the vasculature to provide adequate CBF to activated areas [30]. Neurovascular coupling is closely linked to glutamatergic neurotransmission triggered by synaptically released glutamate and Ca^{2+} influx [31]. It is currently unclear which isoform of Ca^{2+}-dependent constitutive NOS plays the major role in the neurovascular coupling response. While reports indicate the participation of nNOS in transmitting the perfusion response to neuronal stimulus [32,33], eNOS is involved in cerebral autoregulation that plays a defining role in modulating vessel dilatation [34].

L-ornithine and agmatine are the metabolites of L-arginine by arginase and arginine decarboxylase (ADC), respectively (Fig. 1) [12]. They can be metabolized by ornithine decarboxylase (ODC) and agmatinase respectively to produce the polyamines putrescine, spermidine and spermine (Fig. 1), which are essential for maintaining normal cellular function [35]. L-ornithine can also be channelled to produce glutamate, which is further metabolized by glutamine synthetase (GS) or glutamic acid decarboxylase to generate glutamine or γ-aminobutyric acid (GABA) respectively (Fig. 1) [12]. Agmatine is considered as a putative neurotransmitter, participates in learning and memory processes and plays a critical role in regulating the production of NO and polyamines [36–40]. Earlier research has reported altered arginase, ODC and GS expression and polyamine, glutamate and GABA tissue concentrations in AD brains [41–45].

Currently AD has no cure and the amyloid cascade hypothesis has been increasingly challenged [3]. There is therefore an urgent need to explore other mechanisms that contribute to the disease development. Chronic cerebral hypoperfusion (largely due to cerebrovascular eNOS dysfunction) has been suggested to trigger the neurodegenerative processes in AD, particularly for the > 95% of sporadic late-onset cases [3,4,46]. Given the evidence implicating altered L-arginine metabolism in the neuropathogenesis of AD, the present study was designed to systematically investigate how the brain arginine metabolic profile changed in male and female eNOS deficient mice at 14 months of age. Moreover, we also assessed the effects of eNOS deficiency on animals' general behaviour, CBF and neurovascular coupling (by measuring the blood perfusion response in the Barrel cortex to whisker stimulation [33,47]).

2. Material and methods

2.1. Animals

Male and female $eNOS^{-/-}$ ($Nos3^{tm1Unc}$/J; on the C57BL/6J background) mice were originally obtained from Jackson Laboratories (https://www.jax.org/strain/002684) and crossed, resulting in homozygous $eNOS^{-/-}$ mice. Male and female wildtype (WT; C57BL/6J) and $eNOS^{-/-}$ mice at 14 months of age were group-housed ($13 \times 15 \times 38\,cm^3$) based on sex and genotype, maintained on a 12-h light/dark cycle (lights on at 8 a.m.) and provided *ad libitum* access to food and water. Both male and female WT and $eNOS^{-/-}$ mice were used in Experiment 1, whereas only males were used in Experiment 2. All experimental procedures were carried out in accordance with the regulations of the University of Otago Committee on Ethics in the Care and Use of Laboratory Animals and New Zealand legislation, and comply with ARRIVE (Animal Research: Reporting of In Vivo Experiments) guidelines. Every attempt was made to limit the numbers of animals used and to minimise suffering.

2.2. Chemicals

7-nitroindazole (7-NI; Sigma Aldrich, New Zealand) was dissolved in a solution of 40% dimethyl sulfoxide (DMSO) in water and administered at a dose of 30 mg/kg (0.02 ml/gm) [48,49]. Animals in the vehicle group received only 40% DMSO solution (0.02 ml/gm). The solutions were freshly prepared prior to use and administered intraperitoneally (i.p.).

2.3. Behavioural tests

In Experiment 1, male and female WT (n = 21/sex) and $eNOS^{-/-}$ (19 males and 14 females) mice were behaviourally tested in the Y-maze and open field apparatus (Fig. 2A). Behavioural testing was carried out in a windowless room with a video camera mounted on the ceiling. The extramaze cues (the laboratory furniture, lights and several prominent visual features on the walls, as well as the location of the experimenter) were held constant throughout the entire experiment.

Y-maze was a Y-shaped opaque white maze with three open arms at 120° from each other ($13 \times 15 \times 38\,cm^3$), elevated approximately 60 cm from the floor. The positions of the arms were kept constant

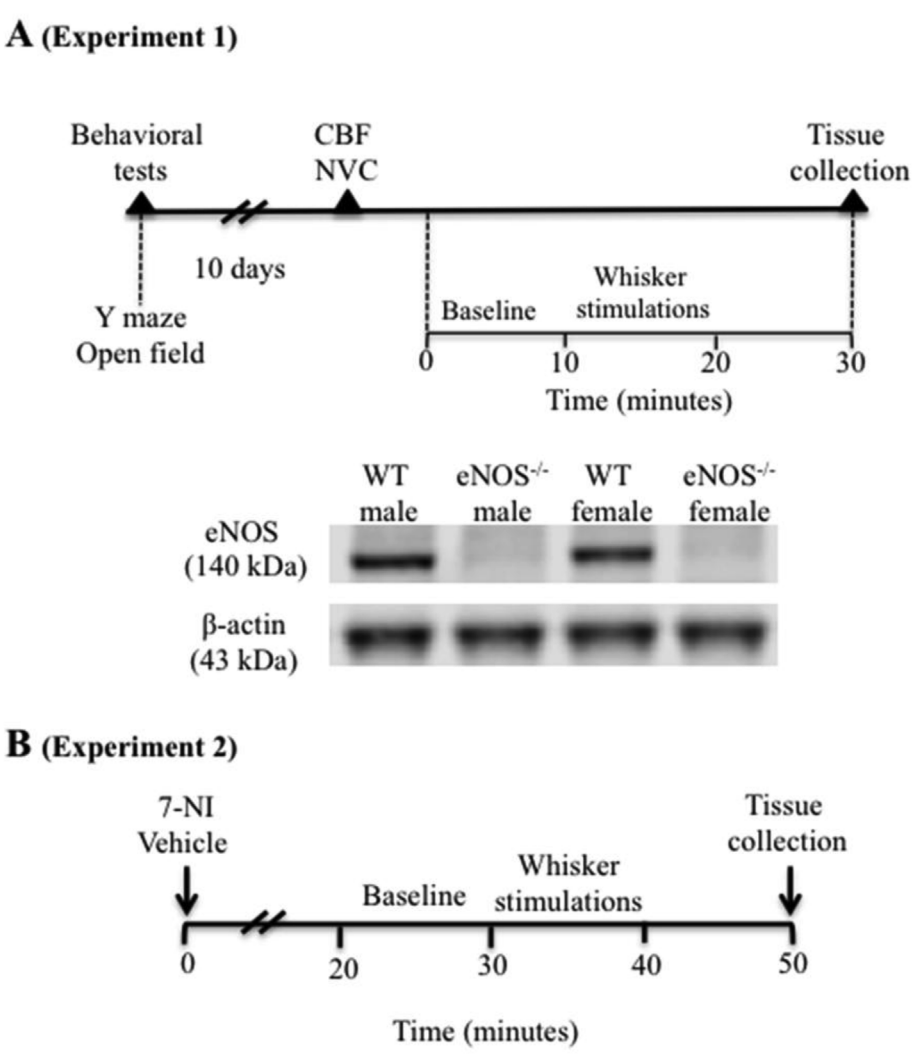

Fig. 2. Experimental timelines. In Experiment 1 (A), male and female wildtype (WT) and eNOS deficient ($eNOS^{-/-}$) mice were tested in the Y-maze and open field, followed by the determinations of the cerebral blood flow (CBF) and neurovascular coupling (NVC; the CBF response to whiskers stimulations) and brain tissue collection. Examples of western blots showing the presence and absence of eNOS protein at 140 kDa in male and female WT and $eNOS^{-/-}$ mice respectively, with the corresponding β-actin bands. In Experiment 2 (B), male WT and $eNOS^{-/-}$ mice were treated with 7-nitroindazole (7-NI) and vehicle followed by the determinations of the CBF and NVC and brain tissue collection.

between animals and groups during the test, with each arm being labelled either A, B or C. Each animal was placed at the centre of the maze facing the same arm and allowed to explore the maze for 7 min. The order of the test was counterbalanced between the four genotype and sex groups. Animals' behaviour was recorded and analyzed offline by a computerized tracking system (TopScan). The number and the sequence of arm entries were recorded. An arm entry was scored when all four paws were in an arm. Alternation behaviour was defined as consecutive entries into all three arms (i.e., ABC, CAB, or BCA but not BAB) [50,51]. The percentage of spontaneous alternation was measured as an index of working memory by calculating the ratio of the actual number of alternations to the possible number (defined as the total number of arm entries minus two) multiplied by 100, i.e., % alternation = [(number of alternations)/(total number of arm entries - 2)] × 100 [52]. The total number of arm entries was measured as an index of locomotor activity.

The open field was an experimental chamber made of opaque white high density plastic, measuring 40 × 40 cm^2 with walls 20 cm high. The box was set up next to the Y-maze and elevated approximately 60 cm from the floor, and animals' general behaviour was then assessed. Each animal was placed into the chamber at the same position and allowed to explore the apparatus freely for 5 min. Again, the order of the test was counterbalanced between the four genotype and sex groups. Animal behaviour was recorded and analyzed offline using TopScan. The total path length travelled, duration of rearings and % time spent in the outer (10 cm from the wall) and inner (central 20 cm^2) zones were analyzed [38,53,54].

2.4. CBF and neurovascular coupling

In Experiment 1, following a 10 day washout period after behavioural testing, baseline CBF and neurovascular coupling were measured in a subset of male and female WT and $eNOS^{-/-}$ mice (n = 8–9/genotype/sex) used for the behavioural testing (Fig. 2A). CBF was measured using a real-time microcirculation imager (PeriCam PSI HR system, Perimed, Sweden), which operates on the Laser Speckle Contrast Analysis Technology (LASCA) and measures blood perfusion in arbitrary Perfusion Units (PU). Mice were anesthetized with isoflurane (4% for initiation and 2% for maintenance) and positioned on a stereotaxic apparatus where body temperature was maintained at 37 °C using a heating pad. A mid-line incision was made to expose the skull and the imager was positioned approximately 10 cm above the brain surface. Baseline perfusion was recorded for 10 min, followed by five 30-s bilateral whisker stimulations using electric toothbrushes with a 90-s inter-stimulation interval [55,56] and a further 10-min recording after the final whisker stimulation (Fig. 2A).

In Experiment 2, the contributions of nNOS to basal CBF and neurovascular coupling were investigated in a separate set of 14 months old male WT (n = 7/treatment group) and $eNOS^{-/-}$ (n = 6/treatment group) mice. After the stable baseline perfusion was obtained, animals were given either 7-NI (30 mg/kg, i.p.) or vehicle (40% DMSO, i.p.) followed by a further 30-min recording. Five 30-s bilateral whisker

stimulations were given 30 min post-treatment, and the whisker stimulation procedure was the same as described above. A further 10-min recording was conducted after the final whisker stimulation (Fig. 2B).

In order to determine the neurovascular coupling response, the Barrel cortex area in each hemisphere was selected as region of interest for each recording on the Pimsoft software (Perimed, Sweded). Change in perfusion response for each stimulation was calculated as a percentage of baseline perfusion, and mean of all 5 stimulations was calculated.

2.5. Tissue collection and preparation

All animals in both experiments were euthanized with pentobarbital (15 mg/ml at a dose of 100 mg/kg), and brains were rapidly removed and left in cold saline (4 °C) for at least 45 s. The frontal cortex (FC), whole hippocampus (HPC), parahippocampal region (PHR) and cerebellum (CE) were dissected freshly on ice from each hemisphere [51,53,57–60]. The brain tissue samples harvested from one hemisphere were weighed, homogenised in ice-cold 10% perchloric acid (~50 mg wet weight per ml) and centrifuged at 10,000 *g* for 10 min to precipitate protein. The perchloric acid extracts (supernatants) were then stored at −80 °C until the high performance liquid chromatographic (HPLC) and liquid chromatography/mass spectrometric (LC/MS) assays. The FC, HPC and CE samples from the other hemisphere were snap-frozen and stored at −80 °C for the enzyme assay and western blotting. In Experiment 1, the brain tissue samples from WT and eNOS$^{-/-}$ mice with (n = 4/genotype/sex group) and without (n = 4/genotype/sex group) CBF tests were used for the following neurochemical assays in order to rule out any procedural effects (such as surgery and isoflurane) on neurochemistry.

2.6. NOS assay

At the time of the protein assay, protease-inhibitory buffer (containing 50 mM Tris-HCL (pH 7.4), 10 μM phenylmethylsulfonyl fluoride, 15 μM pepstatin A and 2 μM leupeptin) was added to each brain tissue sample on ice. The samples were then homogenised and centrifuged at 12,000 *g* for 10 min at 4 °C. Protein concentration in the supernatant was determined using the Bradford method [61]. Each supernatant was then separated into three parts and used for total NOS assay, iNOS assay and Western blot, respectively.

We employed a radioenzymatic assay technique to analyse NOS activity by measuring the ability of tissue homogenates to convert [^{3}H] L-arginine to [^{3}H] L-citrulline in the presence of co-factors as detailed in our previous publications [8,51,53,57,58,60,62–67]. The contribution of iNOS (calcium-independent) to total NOS activity was assessed in the absence of calcium. All assays were performed in duplicate, and the samples from the WT and eNOS$^{-/-}$ groups were counter-balanced. NOS activities were expressed as pmol [^{3}H] L-citrulline/30 min/mg protein.

2.7. Western blot

The protein expression of nNOS, iNOS, eNOS and β-actin in each sample was determined using western blots. The protein concentration in all the samples was equalized to 1 mg/ml. Brain tissue homogenates were mixed with gel loading buffer (containing 50 mM Tris–HCl, 10% SDS, 10% glycerol, 10% 2-mercaptoethanol and 2 mg/ml bromophenol blue) in a ratio of 1:1 and then boiled for 5 min. 10 μL of each sample was loaded in each well on a Bis-Tris Criterion gel (Bio-Rad), and the loading order was counter-balanced between the samples from the four genotype/sex groups for each brain region. Pre-stained protein markers (Bio-Rad) were always run on the same gel [8,58,62,68]. The proteins were allowed to transfer overnight to nitrocellulose membrane (Bio-Rad). The membranes were blocked by incubation in blocking buffer (Bio-Rad) for 6 h, and then incubated with primary polyclonal rabbit antibody raised against iNOS (1:1000, Santa Cruz Biotechnology, sc-651) or monoclonal mouse antibodies raised against eNOS (1:1000, BD Biosciences, 610297) or nNOS (1:5000, Santa Cruz Biotechnology, sc-5302) or β-actin (1:200,000, Santa Cruz Biotechnology, sc-47778), overnight at 4 °C. The membranes were then probed with IRDye® 680RD Goat anti-Mouse IgG antibody or IRDye® 800 CW Donkey anti-Rabbit IgG antibody (1:10,000, LI-COR Biosciences) for 4 h. Detection was performed using Odyssey® CLx Imager (LI-COR, Lincoln, Nebraska, USA). Signals were quantified with Odyssey CLx Image Studio software (LI-COR Biosciences) and normalized by the corresponding β-actin loading controls [8,60,62].

2.8. Amino acid and polyamine analyses

The brain tissue concentrations of amino acids (L-arginine, L-citrulline, L-ornithine, glutamate, glutamine and GABA) and the polyamines spermidine and spermine were quantified by HPLC, while agmatine and putrescine levels were measured by a highly sensitive LC/MS/MS method [8,51,57,58,60,62,69]. High-purity external and internal standards were used (Sigma, Sydney, Australia). All other chemicals were of analytical grade. The samples from both male and female WT and eNOS$^{-/-}$ mice were assayed at the same time in a counterbalanced manner, and the experimenters were blind to the grouping information. The assays were performed in duplicate. The concentrations of L-arginine and its eight downstream metabolites in the tissue were calculated with reference to the peak area of external standards, and values were expressed as μg/g wet tissue [8,51,57,58,60,62,69].

2.9. Statistical analysis

Data were analyzed using two-way analysis of variance (ANOVA) followed by post-hoc tests. Statistical analysis was performed using Graphpad Prism software, and the level of significance was set at $p \leq 0.05$ for all comparisons [70].

3. Results

3.1. Animal genotype

In the present study, the genotype of animals was confirmed by the presence of eNOS protein using western blot. Fig. 2A illustrates a representative immunoblot of eNOS at 140 kDa in WT, but not eNOS$^{-/-}$ mice (Experiment 1).

3.2. Behavioural results

Fig. 3 presents the performance of male and female WT and eNOS$^{-/-}$ mice in the Y-maze and open field tests. For the Y-maze, there were significant effects of genotype ($F(1,71) = 7.98$, $p = 0.006$) and sex ($F(1,71) = 8.35$, $p = 0.005$), but not their interaction, in terms of the total number of arm entries, with more entries in female WT mice relative to female eNOS$^{-/-}$ mice and male WT mice (all $p < 0.05$; Fig. 3A). When % spontaneous alternation was analyzed, there was a significant effect of sex ($F(1,71) = 4.49$, $p = 0.038$), but not genotype or interaction, with an overall pattern of higher values in the males relative to the females (Fig. 3B).

For the open field, when the path length travelled in the apparatus was analyzed, there were significant effects of genotype ($F(1,71) = 4.48$, $P = 0.038$) and sex ($F(1,71) = 9.55$, $P = 0.0029$), but not their interaction, with the longer path generated by the males and WT mice relative to the females and eNOS$^{-/-}$ mice respectively (Fig. 3C). For the duration of rearings, we found a highly significant genotype effect ($F(1,71) = 19.26$, $P < 0.0001$), but not sex or interaction, with the shorter duration in male and female eNOS$^{-/-}$ mice relative to their sex-matched WT controls (all $p < 0.05$, Fig. 3D). There were no significant effects of genotype, sex and their interaction in %

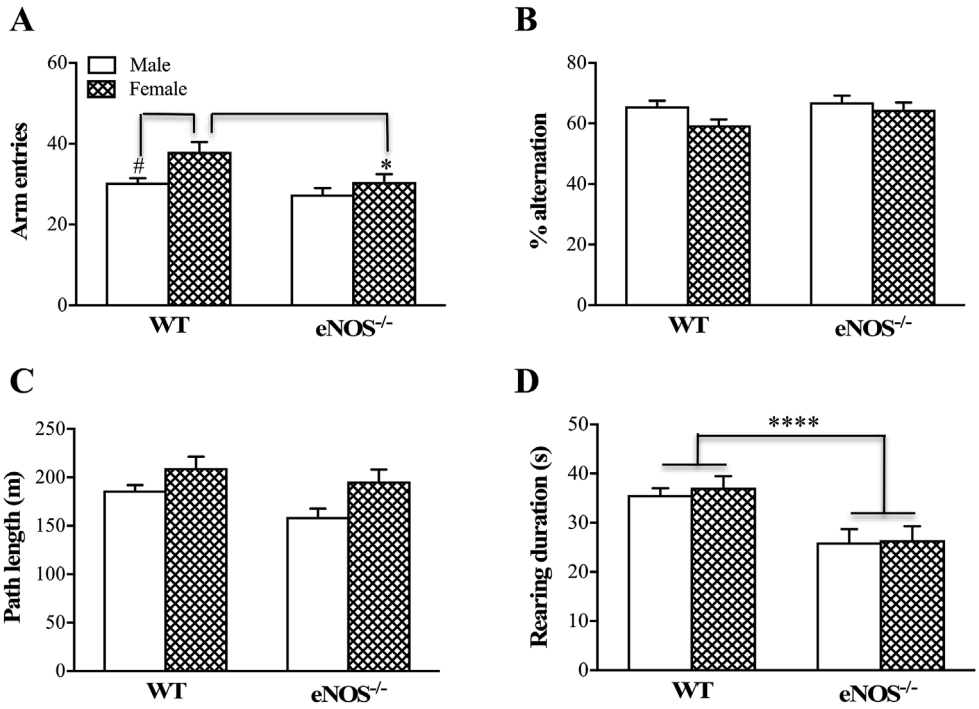

Fig. 3. Animals' performance in the Y-maze and open field. Mean (± SEM) arm entries (A) and % alternation (B) in Y-maze, and path length (m) generated (C) and duration of rearings (s; D) in the open field in male and female WT (n = 21/sex) and eNOS$^{-/-}$ (19 males and 14 females) mice. * indicates a significant difference between sex-matched genotype groups at * p < 0.05 and ****p < 0.0001. # indicates a significant difference between sexes within the same genotype group at p < 0.05.

time spent in the outer or inner zone (data not shown), with all animals spending about 70% of the total time in the outer zone.

3.3. CBF and neurovascular coupling

Experiment 1 determined the changes in basal CBF and perfusion response to whisker stimulation (neurovascular coupling) in the Barrel cortex of 14-month WT and eNOS$^{-/-}$ mice at both sexes. We found a significant effect of sex ($F(1,39) = 13.57$, $P = 0.0007$), but not genotype or interaction, in terms of the basal CBF measurement with the higher value in the females (eNOS$^{-/-}$ mice in particular) relative to the males (Fig. 4A). When the mean perfusion response over 5 whisker stimuli against the baseline perfusion was calculated, there was a highly significant effect of genotype ($F(1,29) = 38.02$, $p < 0.0001$), but not sex or interaction, with the higher responses in eNOS$^{-/-}$ mice relative to their sex-matched WT mice (Fig. 4B).

Experiment 2 investigated whether nNOS contributed to the maintenance of basal CBF and increased perfusion responses in the Barrel cortex to bilateral whisker stimulations in eNOS$^{-/-}$ mice at 14 months of age using a selective nNOS inhibitor 7-NI (30 mg/kg, i.p.). Since there was no sex-difference in neurovascular coupling (Experiment 1), only male WT and eNOS$^{-/-}$ mice were used. Regarding the basal CBF, there was a significant effect of treatment ($F(1,30) = 5.32$, $p = 0.029$), but not genotype or interaction, with the lower values in 7-NI treated mice relative to the vehicle treated mice regardless of genotype (Fig. 4C). When the mean perfusion response in the Barrel cortex over 5 whisker stimuli against baseline perfusion was calculated in each genotype and treatment group, again there was a treatment effect ($F(1,21) = 4.46$, $p = 0.047$), but not genotype or interaction, with significantly reduced response in the eNOS$^{-/-}$ 7-NI group relative to the eNOS$^{-/-}$ vehicle group (Fig. 4D).

3.4. NOS activity and protein expression

Fig. 5A illustrates total NOS activities in the FC, HPC and CE of male and female WT and eNOS$^{-/-}$ mice at 14 months of age (Experiment 1). The radioenzymatic assay revealed no significant effects of genotype, sex and their interaction in the FC and HPC. For CE, there was a significant effect of sex ($F(1,28) = 15.49$, $p = 0.0005$), but not genotype and interaction, with lower NOS activity in the females relative to the males regardless of genotype. iNOS activity was undetectable in all three regions examined.

We further investigated how nNOS and iNOS protein expression levels changed in the FC, HPC and CE under the condition of eNOS deficiency using western blot. There were no significant effects of genotype, sex and their interaction in terms of nNOS protein expression in all three regions (Fig. 5B). iNOS protein was undetectable in all three regions of male and female WT and eNOS$^{-/-}$ mice.

3.5. L-arginine and its downstream metabolites

The HPLC and LC/MS assays were employed to quantify the tissue concentrations of L-arginine and its downstream metabolites in the FC, HPC, PHR and CE of 14-month WT and eNOS$^{-/-}$ mice at both sexes (Experiment 1). For L-arginine (Fig. 6A), while no significant effects of genotype, sex and their interaction were found in the FC, there was a significant effect of sex (HPC: $F(1,28) = 14.11$, $p = 0.0008$; PHR: $F(1,28) = 7.74$, $p = 0.0096$; CE: $F(1,28) = 6.14$, $p = 0.02$), but not genotype or interaction, with the lower levels in the females relative to the males regardless of genotype. For L-citrulline (Fig. 6B), we found no significant effects of genotype, sex and their interaction in the FC and CE. There was however a significant effect of sex ($F(1,28) = 4.36$, $P = 0.046$), but not genotype or interaction, in the HPC with the higher levels in male eNOS$^{-/-}$ mice relative to the females. Regarding the PHR, there was a significant genotype and sex interaction ($F(1,28) = 4.34$, $P = 0.047$), but not genotype or sex effect. For L-ornithine (Fig. 6C), in the FC and PHR, we observed a significant effect of sex (FC: $F(1,28) = 18.01$, $p = 0.0002$; PHR: $F(1,28) = 4.99$, $P = 0.034$), but not genotype or interaction, with the lower levels in the females regardless of genotype. In the HPC and CE, there were significant effects of genotype (HPC: $F(1,28) = 5.59$, $p = 0.026$; CE: $F(1,28) = 4.95$, $p = 0.034$) and sex (HPC: $F(1,28) = 25.41$, $p < 0.0001$; CE: $F(1,28) = 20.26$, $p = 0.0001$), but not interaction, with the higher levels in male eNOS$^{-/-}$ mice relative to male WT mice and the female eNOS$^{-/-}$ mice. Regarding glutamine in all 4 regions (Fig. 6D), there was a significant effect of genotype (FC: $F(1,27) = 11.45$, $p = 0.0022$; HPC: $F(1,27) = 9.35$, $p = 0.005$; PHR: $F(1,27) = 10.04$, $p = 0.0038$; CE: $F(1,27) = 8.45$, $P = 0.0072$), but not sex or interaction, with the lower

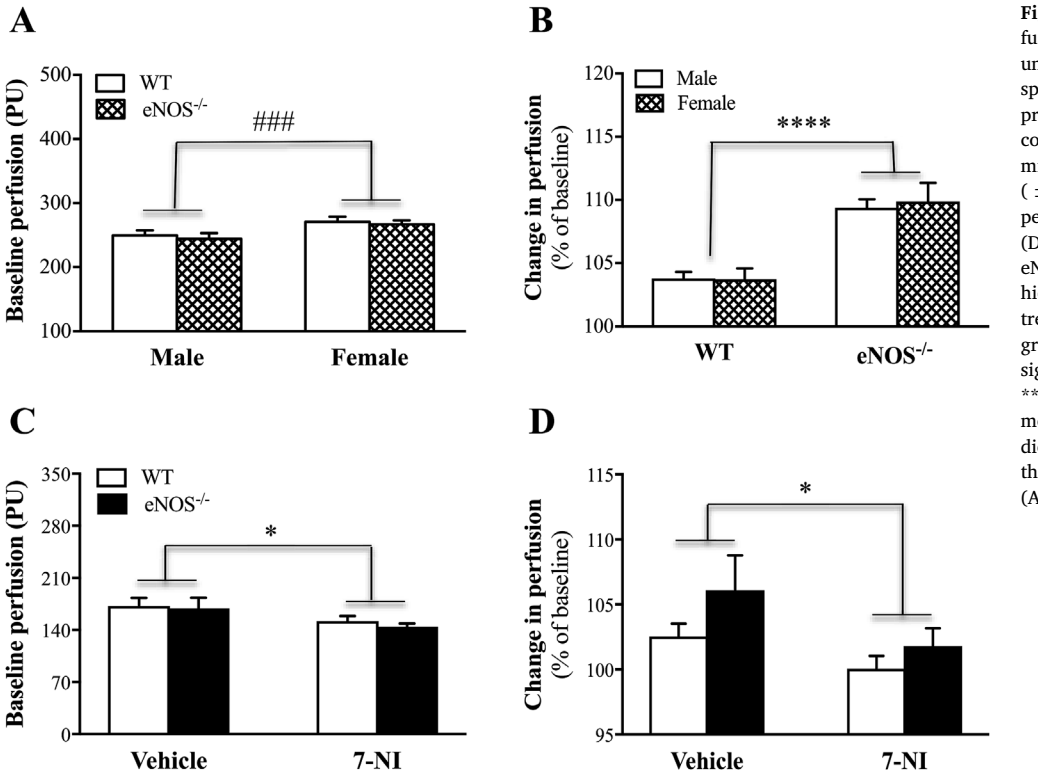

Fig. 4. Mean (± SEM) baseline blood perfusion (A; expressed as arbitrary perfusion units, PU) and change in perfusion in response to whisker stimulations (B; expressed as % of baseline) in the Barrel cortex of male and female WT and eNOS$^{-/-}$ mice (n = 8/genotype/sex/group). Mean (± SEM) baseline blood perfusion (C) and perfusion responses to whisker stimulations (D) in the Barrel cortex of male WT and eNOS$^{-/-}$ mice under the condition of vehicle or 7-nitroindazole (7-NI; 30 mg/kg) treatment (n = 6–7/genotype/treatment group). See text for details. * indicates a significant genotype difference at $^{****}p < 0.0001$ (B) or a significant treatment effect at $^{*}p < 0.05$ (C and D). $^{\#}$ indicates a significant sex difference within the same genotype group at $^{\#\#\#}p < 0.001$ (A).

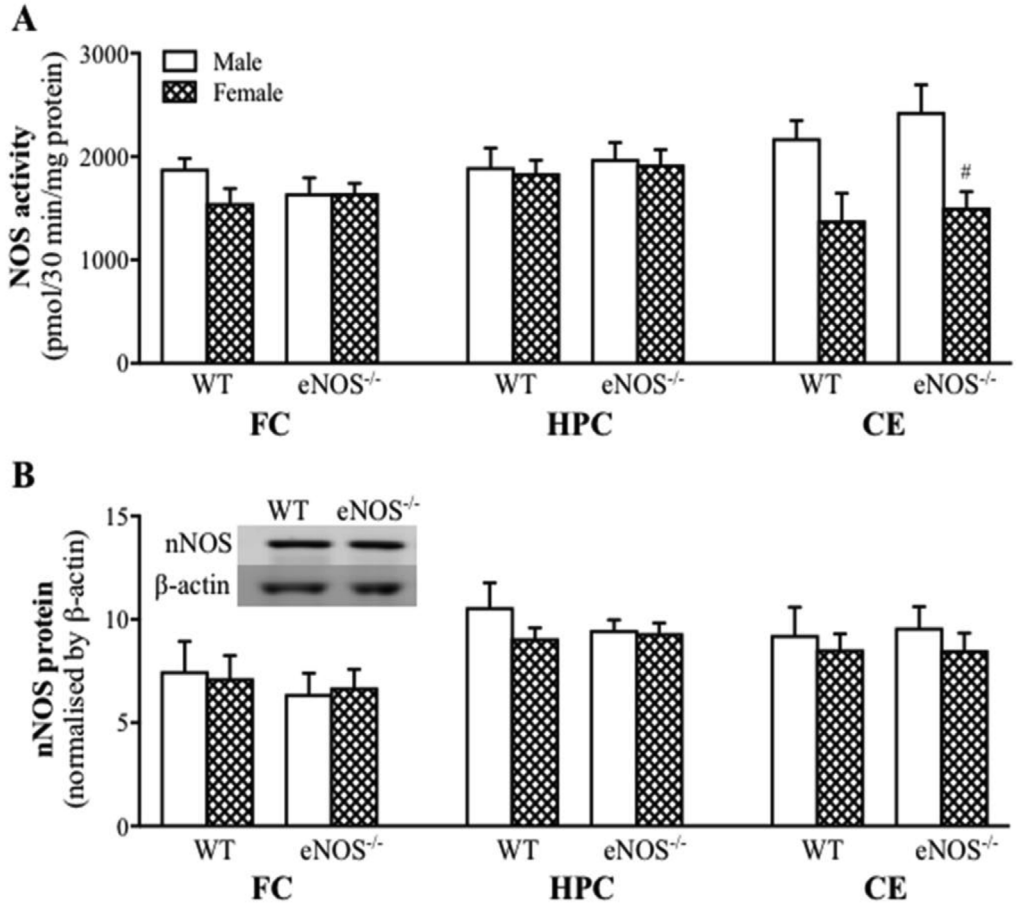

Fig. 5. Mean (± SEM) total NOS activity (A) and nNOS protein expression (B; with representative nNOS and β-actin blots) in the frontal cortex (FC), hippocampus (HPC) and cerebellum (CE) of male and female WT and eNOS$^{-/-}$ mice (n = 8/genotype/sex group).

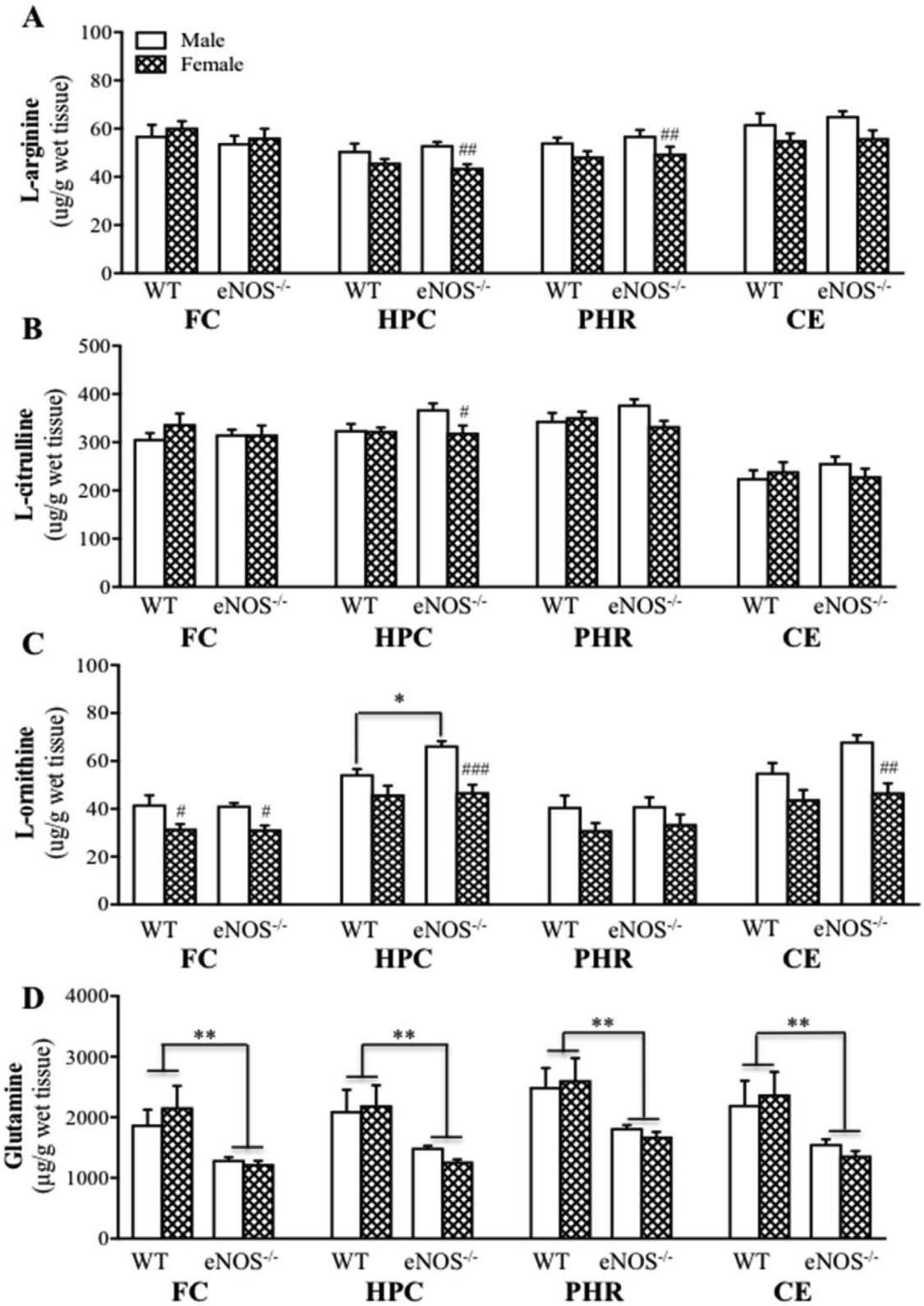

Fig. 6. Mean (± SEM) L-arginine (A), L-citrulline (B), L-ornithine (C) and glutamine (D) levels in the frontal cortex (FC), hippocampus (HPC), parahippocampus (PHR) and cerebellum (CE) of male and female WT and eNOS$^{-/-}$ mice (n = 8/genotype/sex group). * indicates significant difference between genotypes at * $p < 0.05$ or ** $p < 0.01$. # indicates a significant difference between sexes within the same genotype group at $^{\#}p < 0.05$, $^{\#\#}p < 0.01$ or $^{\#\#\#}p < 0.001$.

levels in eNOS$^{-/-}$ mice regardless of sex. For both glutamate and GABA, there were no significant effects of genotype, sex and their interaction in any regon examined (data not shown). For agmatine (Fig. 7A), we found significant effects of genotype ($F(1,27) = 6.73$, $p = 0.015$) and sex ($F(1,27) = 11.05$, $p = 0.0026$), but not interaction, in the PHR with the higher levels in male eNOS$^{-/-}$ mice relative to male WT mice and female eNOS$^{-/-}$ mice. There were no significant effects at all for the other three regions. For putrescine (Fig. 7B), we observed a significant

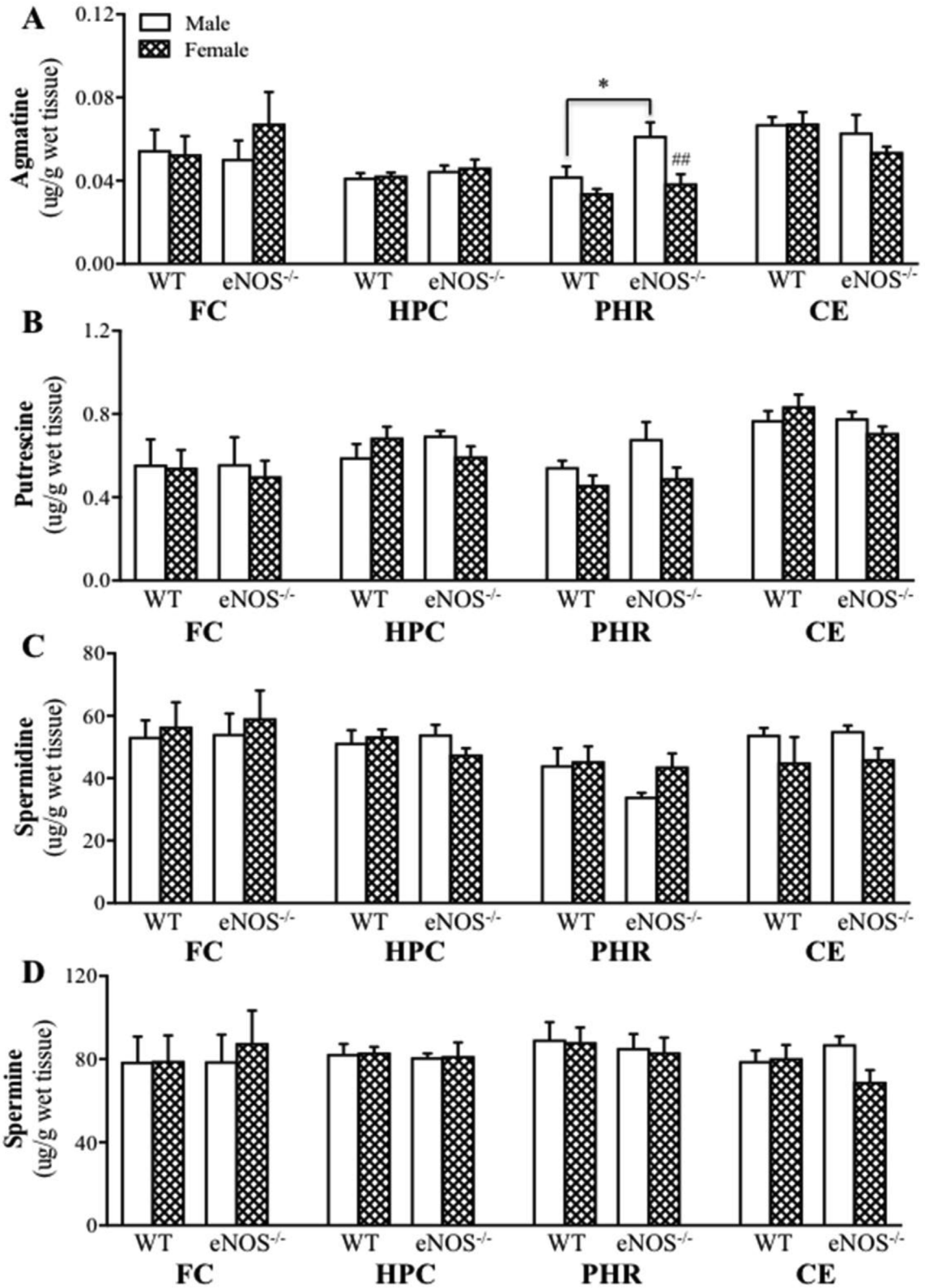

Fig. 7. Mean (± SEM) agmatine (A), putrescine (B), spermidine (C) and spermine (D) levels in the frontal cortex (FC), hippocampus (HPC), parahippocampus (PHR) and cerebellum (CE) of male and female WT and eNOS$^{-/-}$ mice (n = 8/genotype/sex group). * indicates significant difference between genotypes at $p < 0.05$. $^{\#\#}$ indicates a significant difference between sexes within the same genotype group at $p < 0.01$.

effect of sex ($F(1,28) = 6.20$, $p = 0.019$), but not genotype or interaction, in the PHR with a general trend of lower levels in the females regardless of genotype, and a significant interaction ($F(1,27) = 5.32$, $p = 0.029$) in the CE. There were no significant effects at all in the FC and HPC. For both spermidine (Fig. 7C) and spermine (Fig. 7D), there were no significant effects of genotype, sex and their interaction in all four regions examined.

4. Discussion

The gaseous signaling molecule NO is a key mediator of cerebral hemodynamics and contributes significantly to functional hyperemia upon neuronal activation (neurovascular coupling). Altered L-arginine metabolism with reduced eNOS expression has been documented in the AD brain [8,11,20]. Furthermore, eNOS deficient mice show memory deficits, altered APP processing and tau phosphorylation, and increased amyloid beta in the brain [26,27,71], indicating a critical role of loss of eNOS-derived NO in the pathogenesis of AD. The present study demonstrates altered brain arginine metabolism (glutamine in particular), along with behavioural and neurovascular coupling changes, in both male and female eNOS$^{-/-}$ mice at 14 months of age.

4.1. Behavioural impairments in eNOS$^{-/-}$ mice

Rodents naturally explore a less recently visited arm in the Y-maze, and the total number of arm entries and spontaneous alternation reflect animals' locomotor activity and spatial working memory respectively [50]. The open field is a commonly used test to analyse rodents' exploratory and locomotion behaviour based on their natural conflict between exploration of and aversion against bright open areas in a novel environment [72]. In the present study, both male and female eNOS$^{-/-}$ mice made fewer arm entries in the Y maze and travelled shorter distance in the open field apparatus relative to their sex-matched WT mice. These findings indicate reduced locomotion in eNOS$^{-/-}$ mice at both sexes at 14 months of age, which is consistent with an earlier study using 18–22 month eNOS$^{-/-}$ mice [73]. It has been shown that N^{G}-nitro-L-arginine methyl ester (L-NAME; a non-specific NOS inhibitor) resulted in reduced total path length travelled in a novel activity cage in adult Wistar rats [74], supporting a role of NO in locomotion. While spontaneous alternation in the Y maze is a measure of spatial working memory in rodents [75–77], the present study did not find a significant genotype difference in this measurement. Time spent in the centre and/or periphery of the open field apparatus is regarded as an index of anxiety [72]. In the present study, all animals spent about 70% of the total time in the outer zone with no significant genotype difference. It has been shown that exploratory activity represents the ability of animals to integrate spatial features into representation of a novel environment [78]. We found significantly reduced rearings in eNOS$^{-/-}$ mice regardless of sex, which is akin to previous reports [73,74].

It is of interest to note the significant effects of sex in the Y-maze and open field tests. The females tended to make lower percentage of spontaneous alternation and more arm entries in the Y maze and to generate longer path length in the open field when compared to the males. These findings are consistent with an earlier study showing increased locomotor activity, but reduced spontaneous alternation, in the open field and Y-maze tests, in female C57BL/6J mice relative to the males [79]. A large body of evidence has suggested that female rodents are more active than males, possibly due to the influence of sex hormones [80,81].

4.2. Altered neurovascular coupling in eNOS$^{-/-}$ mice

Optimal cerebral blood supply (controlled by CBF) is essential for proper brain function, and NO derived from eNOS plays a critical role in maintaining normal CBF [82]. In Experiment 1, we determined the changes in basal CBF and perfusion response to whisker stimulation (neurovascular coupling) in the Barrel cortex of male and female WT and eNOS$^{-/-}$ mice at 14 months of age. While there was no genotype difference in basal CBF, a significant sex effect was observed with the higher levels in the females relative to the males. Previous human studies have reported higher levels of cerebral blood perfusion in females, which could be due to lower brain weight and higher metabolic rate in women along with other factors, such as heart rate, pulse pressure and hormonal control of CBF [83–85].

In the brain, neuronal activation triggers a local increase of CBF. The integrity of this so-called neurovascular coupling is an essential homeostatic mechanism to adequately adjust the regional CBF based on local neuronal activity [31]. It has been shown that non-selective NOS inhibitors, such as N^{G}-nitro-L-arginine (L-NNA) or L-NAME, reduced neurovascular coupling, suggesting the involvement of NO in mediating the neurovascular coupling response [33,86–88]. Using a laser Doppler probe positioned above the Barrel cortex, Toth et al. reported significantly attenuated CBF change in response to whisker stimulation in 3-month eNOS$^{-/-}$ mice relative to their age-matched WT controls [89]. Surprisingly, the present study found a markedly increased CBF response to whisker stimulations in eNOS$^{-/-}$ mice at 14 months of age regardless of sex and our recent preliminary study observed the exact same pattern in eNOS$^{-/-}$ mice at 4 months of age, which obviously contradicts the earlier report. It should be noted that there are some procedural differences between the two studies. In the study of Toth et al., for example, animals were anesthetized with α-chloralose (50 mg/kg) plus urethane (750 mg/kg) and the contralateral whiskers were stimulated for 1 min at 5 Hz from side to side, with changes in CBF being assessed in three trials divided by 5–10 min intervals [89]. In the present study, however, animals were anesthetized with isoflurane (4% for initiation and 2% for maintenance) and given five trials of robust bilateral whisker stimulations (30 s/trial with 90-s inter-trial intervals) using electric toothbrushes. Low et al. reported a substantial drop in heart rate and blood pH with severe hypercapnia (elevated blood CO_2) in α-chloralose treated mice, but not in isoflurane-treated animals [90]. Isoflurane is a commonly used inhalational anesthetic for the rodent brain imaging experiments [91,92], and can interfere with normal physiology of subjects causing CBF increase [93,94]. Hence different anesthetics and whisker stimulation protocols may contribute to the discrepancy in neurovascular coupling response between the two studies. There is a growing evidence indicating altered neurovascular coupling in ageing and AD [95,96]. While some studies reported attenuated regional CBF during activation in patients and animal models of AD [97–99], increased retinal arterial reaction to flickering light (another way of measuring neurovascular coupling) was found in patients with Alzheimer's dementia relative to healthy controls [100].

Experiment 2 was designed to investigate whether nNOS contributed to the maintenance of basal CBF and increased perfusion responses to bilateral whisker stimulations under the condition of complete eNOS deficiency using a selective nNOS inhibitor. 7-NI treatment reduced the basal CBF levels (12–14% reduction) in 14 months old mice regardless of genotype, which is consistent with earlier research showing reduced blood flow in multiple brain regions in 7-NI treated rats [101,102]. Moreover, 7-NI treatment significantly blocked the increased CBF response to whisker stimulations in eNOS$^{-/-}$ mice, indicating a role of nNOS in mediating such abnormal neurovascular coupling response under the condition of eNOS deficiency. NO is thought to be the link between neuronal and vascular communication, and nNOS is the key isoform mediating the neurovascular coupling response [32,103]. Whisker stimulation activates neurons in the Barrel cortex and leads to glutamate release. Ca^{2+} influx through NMDA receptors influences nNOS activity, hence the biosynthesis of NO [104,105]. As a gaseous retrograde messenger, nNOS-derived NO acts pre-synaptically to regulate glutamate release [106], but also dilates the vessel [107]. As described in a recent mathematical model on the contribution of NO to neurovascular coupling [108], arteriolar radius is an extremely important factor in the CBF response to stimulation, as it directly influences blood perfusion. Meng at al reported nNOS-dependent relaxation in pial arterioles of eNOS knockout mice, indicating the possibility of increased nNOS activity as a compensatory mechanism under the condition of eNOS deficiency [109]. The overall lack of genotype differences in total NOS activities observed in the present study suggests this may be the case (Fig. 5A). Alternatively, the lack of eNOS protein could make the endothelium more sensitive to the surplus

release of nNOS-derived NO induced by whisker stimulations, hence causing sustained vasodilation. This may also explain why nNOS inhibition by 7-NI affected the perfusion response to whisker stimulations in eNOS$^{-/-}$ mice more than WT mice.

It should be pointed out that the reduction in perfusion response to whisker stimulations with 7-NI treatment was small (under 10%; Experiment 2), which suggests that in addition to nNOS-derived NO there must be other factors mediating neurovascular coupling response. Neurovascular coupling is a complex and dynamic brain function. It has been documented that a multitude of factors, such as local extracellular pH, metabolic messengers like adenosine and lactate, cyclooxygenase-2 (COX-2) mediated release of prostaglandins and glutamatergic signaling in astrocytes, are involved in this phenomenon [31]. An earlier study reported increased COX-2 expression in eNOS$^{-/-}$ mice [110], which may contribute to vasodilation in these mice. At present, it is unclear how other factors are affected by eNOS deficiency, which remains to be investigated in the future.

4.3. Altered brain arginine metabolism in eNOS$^{-/-}$ mice

The present study further investigated how the brain L-arginine metabolic profile changed in 14-month male and female mice with eNOS deficiency using the brain tissue samples from WT and eNOS$^{-/-}$ mice with and without CBF tests (Experiment 1). For each neurochemical variable, the mean was very close between animals with and without CBF tests in a given group (data not shown), suggesting the lack of procedural effects (such as isoflurane and surgery) on neurochemistry under the present experimental conditions.

We found no genotype difference in the total NOS activity in the FC, HPC and CE regions, however a significant sex-difference in the CE with a 37% reduction in the females. Since iNOS activity and protein expression in the brain were undetectable in both genotypes, we speculate that nNOS may be responsible for the maintenance of NOS activity in eNOS$^{-/-}$ mice. It is of interest to note that Hara et al. also reported a lack of difference in NOS activity between WT and eNOS$^{-/-}$ mice [111], indicating a compensatory mechanism to maintain the total NOS activity in eNOS$^{-/-}$ mice. Son et al. compared the total NOS activity changes in the hippocampus between eNOS$^{-/-}$, nNOS$^{-/-}$ and doubly mutant eNOS$^{-/-}$/nNOS$^{-/-}$ mice [112]. In comparison with WT mice, there were slightly increased NOS activity in eNOS$^{-/-}$ mice, but significantly decreased NOS activities in nNOS$^{-/-}$ and eNOS$^{-/-}$/nNOS$^{-/-}$ mice. These findings suggest a major contribution of nNOS to the total NOS activity in the hippocampus and a likely compensatory up-regulation of nNOS in eNOS$^{-/-}$ mice [112]. In the present study, however, there were no genotype and sex differences in nNOS protein expression in the FC, HPC and CE. It has been shown that the expression or synthesis of NOS proteins can be regulated independently of their activity and there is a post-transcriptional regulation of nNOS expression [113,114].

We then quantified the levels of L-arginine and its downstream metabolites in the FC, HPC, PHR and CE regions in 14 months old WT and eNOS$^{-/-}$ mice at both sexes. While there were no significant genotype differences in L-arginine and L-citrulline in all four regions examined, some sex differences were noted with females having lower levels of L-arginine in these regions and reduced L-citrulline in the HPC relative to the males. It has been documented that female eNOS$^{-/-}$ mice display dysfunctional ovarian cyclicity and morphology and altered steroidogenesis [115,116], indicating an important role of eNOS-derived NO in female reproductive cycle. Regarding L-ornithine (the product of arginase), we found a significant effect of sex in the FC and PHR with the lower levels in the females regardless of genotype. Moreover, there were significant effects of genotype and sex in the HPC and CE, with higher levels of L-ornithine in male eNOS$^{-/-}$ mice relative to male WT mice (perhaps due to the upregulation of arginase) and lower levels in the females when compared to the males regardless of genotype.

L-ornithine can be metabolized to glutamate and then to glutamine or GABA. While there were no significant genotype and sex differences in glutamate or GABA in all four brain regions examined, intriguingly we observed a marked decrease in glutamine in eNOS$^{-/-}$ mice regardless of sex or brain region. In the brain, phosphate-dependent glutaminase (PAG) convers glutamine to glutamate and ammonia in neurons. Glutamate is then taken up into astrocytes after being released from the synaptic terminals and converted (along with ammonia) into glutamine by GS, and glutamine is then transported to the neurons and reused to generate glutamate [117]. This so-called glutamate-glutamine cycle is an important constituent of the glutamatergic neurotransmission system and serves myriad functions such as regeneration of glutamate in the neurons and removal of excess glutamate from synapse preventing excitotoxicity and most importantly to detoxify ammonia resulting from brain amino acid catabolism [118,119]. Currently, it is unclear what (PAG or GS) contributes to reduced brain tissue content of glutamine in eNOS$^{-/-}$ mice. There is evidence showing that excessive amount of NO derived from nNOS can reduce GS activity [120,121] and glutamine level changes can influence the generation of NO and L-arginine from L-citrulline in endothelial cells [122].

It is of interest to note that the glutamate-glutamine cycle is profoundly impaired in the AD brain, for example with reduced GS expression and a negative correlation between GS and Aβ deposits [123]. Given its role in the detoxification of ammonia in the brain, GS dysfunction (hence reduced glutamine levels) may result in the accumulation of ammonia, which is well documented in AD [124–126]. It should be noted that L-ornithine can also be converted to L-citrulline by ornithine transcarbamylase (OTC), and L-citrulline can be recycled to produce L-arginine via argininosuccinate synthetase (ASS) and argininosuccinate lyase (ASL) (Fig. 1) [12,127]. OTC, ASS, ASL and arginase, along with carbamoyl phosphate synthetase-I (CPS-I), are the five enzymes of the urea cycle, which dispose of toxic ammonia in the nontoxic and readily excretable form of urea (Fig. 1) [127]. There is evidence suggesting the presence of the complete urea cycle in the AD brain, which is likely a compensatory mechanism to remove excessive ammonia [42,128]. Future research is required to understand the underlying mechanisms and functional significance of the observed glutamine reduction in eNOS$^{-/-}$ mice by focusing on the urea cycle.

Polyamines putrescine, spermidine and spermine can be formed by ODC from L-ornithine and by agmatinase from agmatine (decarboxylated arginine) [35]. In the present study, we found higher levels of agmatine in male eNOS$^{-/-}$ mice relative to male WT mice and female eNOS$^{-/-}$ mice, and a general trend of lower levels of putrescine in the females relative to the males, in the PHR, with no genotype and sex differences in spermidine and spermine in any region examined. Agmatine is a putative neurotransmitter, participates directly in learning and memory processes, interacts with NMDA, imidazoline and α_2-adrenergic receptors, and regulates the production of NO and polyamines [129–131]. Therefore, altered agmatine levels with genotype and sex may have important functional significance, which needs to be addressed in future research.

In summary, the present study demonstrates the genotype- and/or sex-related changes in behavioural function, basal CBF, neurovascular coupling and brain L-arginine metabolism in mice with complete eNOS deficiency at 14 months of age. A small, but significant, blockage of increased CBF responses following whisker stimulations in eNOS$^{-/-}$ mice by 7-NI treatment indicates the involvement of nNOS in mediating the observed abnormal neurovascular coupling although other contributing factors need to be explored in the future. Intriguingly, eNOS$^{-/-}$ mice displayed a marked and global reduction in glutamine regardless of sex. Interestingly, altered neurovascular coupling and reduced glutamine levels in the brain are present in eNOS$^{-/-}$ mice at 4 months of age (unpublished preliminary observations). It has been shown that eNOS$^{-/-}$ mice display altered APP processing and increased Aβ production in the brain with age [26]. There is no global reduction of glutamine in the brain in APP/PS1 mice with chronic Aβ

accumulation [60] or in rats following the intracerebroventricular infusion of aggregated $A\beta_{25-35}$ [63,132]. We therefore speculate that the changes in neurovascular coupling and glutamine metabolism observed in the present study are likely the consequences of loss of eNOS-derived NO rather than age. Given the links of glutamine with the glutamatergic neurotransmission and ammonia/urea cycle, more research is required to understand the mechanisms and functional significance of these changes. It is of interest to note that our preliminary work shows increased urea levels in the cortex of $eNOS^{-/-}$ mice, which merits a future research to systematically investigate how GS and the urea cycle enzymes change in eNOS deficient mice. Since loss of eNOS-derived NO contributes to amyloidogenic processing of APP and cognitive decline [26], eNOS dysfunction and the ensuing cerebrovascular and neurovascular coupling dysfunction and altered neurochemistry may have a significant implication in the neuropathogenesis and/or development of AD.

Declaration of conflict of interest

All authors declared no potential conflict of interest with respect to the research, authorship, and/or publication of this work.

Author contributions

P. Liu, A. Hariharan and H. Zhang designed research; A. Hariharan Y. Jing, N. D. Collie performed research and collected data; A. Hariharan and P. Liu analyzed data, interpreted results and wrote and revised the paper; all authors contributed to the manuscript preparation.

Acknowledgements

This work was supported by the Health Research Council of New Zealand (16/597), New Zealand Lottery Health Research (R-LHR-2016-27043) and University of Otago Research Grant. The authors would like to acknowledge the support of the Department of Anatomy and Hercus Taieri Resource Unit, University of Otago, New Zealand. Ashwini Hariharan is the recipient of the University of Otago Postgraduate Scholarship.

References

[1] J.A. Hardy, G.A. Higgins, Alzheimer's disease: the amyloid cascade hypothesis, Science 256 (1992) 184–185.
[2] G.P. Morris, I.A. Clark, B. Vissel, Inconsistencies and controversies surrounding the amyloid hypothesis of Alzheimer's disease, Acta Neuropathol Commun 2 (2014) 1–21.
[3] D.A. Drachman, The amyloid hypothesis, time to move on: amyloid is the downstream result, not cause, of Alzheimer's disease, Alzheimers Dement 10 (2014) 372–380.
[4] G. Aliev, H.H. Palacios, A.E. Lipsitt, et al., Nitric oxide as an initiator of brain lesions during the development of Alzheimer disease, Neurotox. Res. 16 (2009) 293–305.
[5] J.C. de la Torre, Cerebral hemodynamics and vascular risk factors: setting the stage for Alzheimer's disease, J. Alzheimers Dis. 32 (2012) 553–567.
[6] R.D. Bell, B.V. Zlokovic, Neurovascular mechanisms and blood-brain barrier disorder in Alzheimer's disease, Acta Neuropathol. 118 (2009) 103–113.
[7] A. Law, S. Gauthier, R. Quirion, Say NO to Alzheimer's disease: the putative links between nitric oxide and dementia of the Alzheimer's type, Brain Res. Rev. 35 (2001) 73–96.
[8] P. Liu, M.S. Fleete, Y. Jing, et al., Altered arginine metabolism in Alzheimer's disease brains, Neurobiol. Aging 35 (2014) 1992–2003.
[9] C.G. Whiteley, Arginine metabolising enzymes as targets against Alzheimer's disease, Neurochem. Int. 67 (2014) 23–31.
[10] J. Yi, L.L. Horky, A.L. Friedlich, et al., L-arginine and Alzheimer's disease, Int. J. Clin. Exp. Pathol. 3 (2009) 211–238.
[11] K. Inoue, H. Tsutsui, H. Akatsu, et al., Metabolic profiling of Alzheimer's disease brains, Sci. Rep. 3 (2013) 1–9.
[12] G. Wu, S.M. Morris, Arginine metabolism: nitric oxide and beyond, Biochem. J. 336 (1998) 1–17.
[13] D.S. Bredt, Endogenous nitric oxide synthesis: biological functions and pathophysiology, Free Radic. Res. 31 (1999) 577–596.
[14] R. Feil, T. Kleppisch, NO/cGMP-dependent modulation of synaptic transmission, Handb. Exp. Pharmacol. 184 (2008) 529–560.
[15] A.J. Susswein, N.M. Ayelet Katzoff, I. Hurwitz, Nitric oxide and memory, Neuroscientist 10 (2004) 153–162.
[16] L. Zhou, D.Y. Zhu, Neuronal nitric oxide synthase: structure, subcellular localization, regulation, and clinical implications, Nitric Oxide 20 (2009) 223–230.
[17] J. Zhu, W. Song, L. Li, et al., Endothelial nitric oxide synthase: a potential therapeutic target for cerebrovascular diseases, Mol. Brain 9 (2016) 1–8.
[18] T. Malinski, Nitric oxide and nitroxidative stress in Alzheimer's disease, J. Alzheimers Dis. 11 (2007) 207–218.
[19] S.M. de la Monte, B.X. Lu, Y.K. Sohn, et al., Aberrant expression of nitric oxide synthase III in Alzheimer's disease: relevance to cerebral vasculopathy and neurodegeneration, Neurobiol. Aging 21 (2000) 309–319.
[20] B. Jeynes, J. Provias, Significant negative correlations between capillary expressed eNOS and Alzheimer lesion burden, Neurosci. Lett. 463 (2009) 244–248.
[21] J. Provias, B. Jeynes, Neurofibrillary tangles and senile plaques in Alzheimer's brains are associated with reduced capillary expression of vascular endothelial growth factor and endothelial nitric oxide synthase, Curr. Neurovascular Res. 5 (2008) 199–205.
[22] H.-J. Luth, G. Munch, T. Arendt, Aberrant expression of NOS isoforms in Alzheimer's disease is structurally related to nitrotyrosine formation, Brain Res. 953 (2002) 135–143.
[23] H.-J. Luth, M. Holzer, U. Gartner, et al., Expression of endothelial and inducible NOS-isoforms is increased in Alzheimer's disease, in APP23 transgenic mice and after experimental brain lesion in rat: evidence for an induction by amyloid pathology, Brain Res. 913 (2001) 57–67.
[24] S.A. Austin, L.V. d'Uscio, Z.S. Katusic, Supplementation of nitric oxide attenuates AβPP and BACE1 protein in cerebral microcirculation of eNOS-deficient mice, J. Alzheimers Dis. 33 (2013) 29–33.
[25] S.A. Austin, A.V. Santhanam, Z.S. Katusic, Endothelial nitric oxide modulates expression and processing of amyloid precursor protein, Circ. Res. 107 (2010) 1498–1502.
[26] S.A. Austin, A.V. Santhanam, D.J. Hinton, et al., Endothelial nitric oxide deficiency promotes Alzheimer's disease pathology, J. Neurochem. 127 (2013) 691–700.
[27] S.A. Austin, Z.S. Katusic, Loss of endothelial nitric oxide synthase promotes p25 generation and tau phosphorylation in a murine model of Alzheimer's disease, Circ. Res. 119 (2016) 1–29.
[28] B.T. Hawkins, T.P. Davis, The blood-brain barrier/neurovascular unit in health and disease, Pharmacol. Rev. 57 (2005) 173–185.
[29] C. Iadecola, The neurovascular unit coming of age: a journey through neurovascular coupling in health and disease, Neuron 96 (2017) 17–42.
[30] N. Nicolakakis, E. Hamel, Neurovascular function in Alzheimer's disease patients and experimental models, J. Cereb. Blood Flow Metab. 31 (2011) 1354–1370.
[31] D. Attwell, A.M. Buchan, S. Charpak, et al., Glial and neuronal control of brain blood flow, Nature 468 (2010) 232–243.
[32] C.F. Lourenço, R.M. Santos, R.M. Barbosa, et al., Neurovascular coupling in hippocampus is mediated via diffusion by neuronal-derived nitric oxide, Free Radical Biol. Med. 73 (2014) 421–429.
[33] J. Ma, C. Ayata, P.L. Huang, et al., Regional cerebral blood flow response to vibrissal stimulation in mice lacking type I NOS gene expression, Am. J. Physiol. 270 (1996) 1085–1090.
[34] D.N. Atochin, P.L. Huang, Role of endothelial nitric oxide in cerebrovascular regulation, Curr. Pharmaceut. Biotechnol. 12 (2011) 1334–1342.
[35] H.M. Wallace, A.V. Fraser, A. Hughes, A perspective of polyamine metabolism, Biochem. J. 376 (2003) 1–14.
[36] J.E. Piletz, F. Aricioglu, J.-T. Cheng, et al., Agmatine: clinical applications after 100 years in translation, Drug Discov. Today 18 (2013) 880–893.
[37] D.J. Reis, S. Regunathan, Is agmatine a novel neurotransmitter in brain? Trends Pharmacol. Sci. 21 (2000) 187–193.
[38] P. Liu, N.D. Collie, S. Chary, et al., Spatial learning results in elevated agmatine levels in the rat brain, Hippocampus 18 (2008) 1094–1098.
[39] M. Rushaidhi, Y. Jing, H. Zhang, et al., Participation of hippocampal agmatine in spatial learning: an in vivo microdialysis study, Neuropharmacology 65 (2013) 200–205.
[40] S. Seo, P. Liu, B. Leitch, Spatial learning-induced accumulation of agmatine and glutamate at hippocampal CA1 synaptic terminals, Neuroscience 192 (2011) 28–36.
[41] C.A. Colton, R.T. Mott, H. Sharpe, et al., Expression profiles for macrophage alternative activation genes in AD and in mouse models of AD, J. Neuroinflammation 3 (2006) 1–12.
[42] F. Hansmannel, A. Sillaire, M.I. Kamboh, et al., Is the urea cycle involved in Alzheimer's disease? J. Alzheimers Dis. 21 (2010) 1013–1021.
[43] L.D. Morrison, X.-C. Cao, S.J. Kish, Ornithine decarboxylase in human brain: influence of aging, regional distribution, and Alzheimer's disease, J. Neurochem. 71 (1998) 288–294.
[44] L.D. Morrison, S.J. Kish, Brain polyamine levels are altered in Alzheimer's disease, Neurosci. Lett. 197 (1995) 5–8.
[45] H. Tumani, G. Shen, J. Peter, et al., Glutamine synthetase in cerebrospinal fluid, serum, and brain: a diagnostic marker for Alzheimer disease? Arch. Neurol. 56 (1999) 1241–1246.
[46] J.C. de la Torre, A turning point for Alzheimer's disease? Biofactors 38 (2012) 78–83.
[47] C. Lecrux, E. Hamel, Neuronal networks and mediators of cortical neurovascular coupling responses in normal and altered brain states, Philos. Trans. R. Soc. Lond. B Biol. Sci. 371 (2016) 1–13.
[48] C. Brožíčková, J. Otáhal, Effect of an inhibitor of neuronal nitric oxide synthase 7-nitroindazole on cerebral hemodynamic response and brain excitability in

urethane-anesthetized rats, Physiol. Res. 62 (2013) 57–66.
[49] P.K. Moore, P. Wallace, Z. Gaffen, et al., Characterization of the novel nitric oxide synthase inhibitor 7-nitro indazole and related indazoles: antinociceptive and cardiovascular effects, Br. J. Pharmacol. 110 (1993) 219–224.
[50] M. Sarter, G. Bodewitz, D.N. Stephens, Attenuation of scopolamine-induced impairment of spontaneous alteration behaviour by antagonist but not inverse agonist and agonist beta-carbolines, Psychopharmacology (Berl) 94 (1998) 491–495.
[51] L.T. Knox, Y. Jing, M.S. Fleete, et al., Scopolamine impairs behavioural function and arginine metabolism in the rat dentate gyrus, Neuropharmacology 61 (2011) 1452–1462.
[52] C.J. Miedel, J.M. Patton, A.N. Miedel, et al., Assessment of spontaneous alternation, novel object recognition and limb clasping in transgenic mouse models of amyloid-β and tau neuropathology, J Vis Exp 123 (2017) 1–8.
[53] N. Gupta, Y. Jing, N.D. Collie, et al., Ageing alters behavioural function and brain arginine metabolism in male Sprague-Dawley rats, Neuroscience 226 (2012) 178–196.
[54] M.L. Seibenhener, M.C. Wooten, Use of the open field maze to measure locomotor and anxiety-like behavior in mice, J Vis Exp 96 (2015) 1–6.
[55] P. Papadopoulos, P. Rosa-Neto, J. Rochford, et al., Pioglitazone improves reversal learning and exerts mixed cerebrovascular effects in a mouse model of Alzheimer's disease with combined amyloid-β and cerebrovascular pathology, PLoS One 8 (2013) 1–13.
[56] C. Lecrux, X. Toussay, A. Kocharyan, et al., Pyramidal neurons are “neurogenic hubs” in the neurovascular coupling response to whisker stimulation, J. Neurosci. 31 (2011) 9836–9847.
[57] L.T. Knox, Y. Jing, J. Bawazier-Edgecombe, et al., Effects of withdrawal from repeated phencyclidine administration on behavioural function and brain arginine metabolism in rats, Pharmacol. Biochem. Behav. 153 (2017) 45–59.
[58] P. Liu, S. Chary, R. Devaraj, et al., Effects of aging on agmatine levels in memory-associated brain structures, Hippocampus 18 (2008) 853–856.
[59] P. Liu, Y. Jing, H. Zhang, Age-related changes in arginine and its metabolites in memory-associated brain structures, Neuroscience 164 (2009) 611–628.
[60] D. Bergin, Y. Jing, B. Mockett, et al., Altered plasma arginine metabolome precedes behavioural and brain arginine metabolomic profile changes in the APPswe/PS1ΔE9 mouse model of Alzheimer's disease, Transl. Psychiatry 8 (2018) 1–14.
[61] M.M. Bradford, A rapid and sensitive method for the quantitation of microgram quantities of protein utilizing the principle of protein-dye binding, Anal. Biochem. 72 (1976) 248–254.
[62] P. Liu, Y. Jing, N. Collie, et al., Altered brain arginine metabolism in schizophrenia, Transl. Psychiatry 6 (2016) 1–9.
[63] P. Liu, Y. Jing, N.D. Collie, et al., Pre-aggregated Aβ25–35 alters arginine metabolism in the rat hippocampus and prefrontal cortex, Neuroscience 193 (2011) 269–282.
[64] P. Liu, P.F. Smith, I. Appleton, et al., Potential involvement of NOS and arginase in age-related behavioural impairments, Exp. Gerontol. 39 (2004) 1207–1222.
[65] P. Liu, P.F. Smith, I. Appleton, et al., Age-related changes in nitric oxide synthase and arginase in the rat prefrontal cortex, Neurobiol. Aging 25 (2004) 547–552.
[66] P. Liu, Y. Zheng, P.F. Smith, et al., Changes in NOS protein expression and activity in the rat hippocampus, entorhinal and postrhinal cortices after unilateral electrolytic perirhinal cortex lesions, Hippocampus 13 (2003) 561–571.
[67] P. Liu, P.F. Smith, I. Appleton, et al., Nitric oxide synthase and arginase in the rat hippocampus and the entorhinal, perirhinal, postrhinal, and temporal cortices: regional variations and age-related changes, Hippocampus 13 (2003) 859–867.
[68] M. Rushaidhi, H. Zhang, P. Liu, Effects of prolonged agmatine treatment in aged male Sprague–Dawley rats, Neuroscience 234 (2013) 116–124.
[69] P. Liu, N. Gupta, Y. Jing, et al., Further studies of the effects of aging on arginine metabolites in the rat vestibular nucleus and cerebellum, Neuroscience 348 (2017) 273–287.
[70] J.F. Zolman, Biostatistics: Experimental Design and Statistical Inference, Oxford University Press, Oxford, UK, 1993.
[71] X.L. Tan, Y.Q. Xue, T. Ma, et al., Partial eNOS deficiency causes spontaneous thrombotic cerebral infarction, amyloid angiopathy and cognitive impairment, Mol. Neurodegener. 10 (2015) 1–13.
[72] U. Schmitt, C. Hiemke, Combination of open field and elevated plus-maze: a suitable test battery to assess strain as well as treatment differences in rat behavior, Prog. Neuro-Psychopharmacol. Biol. Psychiatry 22 (1998) 1197–1215.
[73] E. Dere, M.A.D.S. Silva, B. Topic, Aged endothelial nitric oxide synthase knockout mice exhibit higher mortality concomitant with impaired open-field habituation and alterations in forebrain neurotransmitter levels, Genes Brain Behav. 1 (2002) 204–213.
[74] C. Sandi, C. Venero, C. Guaza, Decreased spontaneous motor activity and startle response in nitric oxide synthase inhibitor-treated rats, Eur. J. Pharmacol. 277 (1995) 89–97.
[75] R.M.J. Deacon, J.N.P. Rawlins, T-maze alternation in the rodent, Nat. Protoc. 1 (2006) 7–12.
[76] J.L.W. Yau, K.M. McNair, J. Noble, et al., Enhanced hippocampal long-term potentiation and spatial learning in aged 11β-hydroxysteroid dehydrogenase type 1 knock-out mice, J. Neurosci. 27 (2007) 10487–10496.
[77] Z. Sarnyai, E.L. Sibille, C. Pavlides, et al., Impaired hippocampal-dependent learning and functional abnormalities in the hippocampus in mice lacking serotonin1A receptors, Proc. Natl. Acad. Sci. U. S. A. 97 (2000) 14731–14736.
[78] C. Thinus-Blanc, Animal Spatial Cognition: Behavioural and Brain Approach, World Scientific, Singapore, 1996.
[79] L.B. Tucker, A.H. Fu, J.T. McCabe, Performance of male and female C57BL/6J mice on motor and cognitive tasks commonly used in pre-clinical traumatic brain injury research, J. Neurotrauma 33 (2016) 880–894.
[80] S. Ogawa, J. Chan, J.-Å. Gustafsson, et al., Estrogen increases locomotor activity in mice through estrogen receptor α : specificity for the type of activity, Endocrinology 144 (2003) 230–239.
[81] J.T. Lightfoot, Sex hormones' regulation of rodent physical activity: a review, Int. J. Biol. Sci. 4 (2008) 126–132.
[82] N. Toda, K. Ayajiki, T. Okamura, Cerebral blood flow regulation by nitric oxide: recent advances, Pharmacol. Rev. 61 (2009) 62–97.
[83] R.E. Gur, R.C. Gur, Gender differences in regional cerebral blood flow, Schizophr. Bull. 16 (1990) 247–254.
[84] C. Ghisleni, S. Bollmann, A. Biason-Lauber, Effects of steroid hormones on sex differences in cerebral perfusion, PLoS One 10 (2015) 1–15.
[85] G. Rodriguez, S. Warkentin, J. Risberg, et al., Sex differences in regional cerebral blood flow, J. Cereb. Blood Flow Metab. 8 (1988) 783–789.
[86] F.J. Northington, G.P. Matherne, R.M. Berne, Competitive inhibition of nitric oxide synthase prevents the cortical hyperemia associated with peripheral nerve stimulation, Proc. Natl. Acad. Sci. U. S. A. 89 (1992) 6649–6652.
[87] U. Dirnagl, U. Lindauer, A. Villringer, Role of nitric oxide in the coupling of cerebral blood flow to neuronal activation in rats, Neurosci. Lett. 149 (1993) 43–46.
[88] A.C. Ngai, J.R. Meno, H.R. Winn, L-NNA suppresses cerebrovascular response and evoked potentials during somatosensory stimulation in rats, Am. J. Physiol. 269 (1995) H1803–H1810.
[89] P. Toth, S. Tarantini, A. Davila, et al., Purinergic glio-endothelial coupling during neuronal activity: role of P2Y1 receptors and eNOS in functional hyperemia in the mouse somatosensory cortex, Am. J. Physiol. Heart Circ. Physiol. 309 (2015) H1837–H1845.
[90] L.A. Low, L.C. Bauer, B.A. Klaunberg, Comparing the effects of isoflurane and alpha chloralose upon mouse physiology, PLoS One 11 (2016) 1–14.
[91] K. Masamoto, T. Kim, M. Fukuda, et al., Relationship between neural, vascular, and BOLD signals in isoflurane-anesthetized rat somatosensory cortex, Cerebr. Cortex 17 (2007) 942–950.
[92] E.R. Muir, Q. Shen, T.Q. Duong, Cerebral blood flow MRI in mice using the cardiac-spin-labeling technique, Magn. Reson. Med. 60 (2008) 744–748.
[93] B.F. Matta, K.J. Heath, K. Tipping, et al., Direct cerebral vasodilatory effects of sevoflurane and isoflurane, Anesthesiology 91 (1999) 677–680.
[94] C.X. Li, S. Patel, D.J.J. Wang, et al., Effect of high dose isoflurane on cerebral blood flow in macaque monkeys, Magn. Reson. Imaging 32 (2014) 956–960.
[95] C.F. Lourenço, A. Ledo, C. Dias, et al., Neurovascular and neurometabolic derailment in aging and Alzheimer's disease, Front. Aging Neurosci. 7 (2015) 1–8.
[96] S. Tarantini, C.H.T. Tran, G.R. Gordon, et al., Impaired neurovascular coupling in aging and Alzheimer's disease: contribution of astrocyte dysfunction and endothelial impairment to cognitive decline, Exp. Gerontol. 94 (2017) 52–58.
[97] S. Rombouts, F. Barkhof, D. Veltman, et al., Functional MR imaging in Alzheimer's disease during memory encoding, AJNR Am J Neuroradiol 21 (2000) 1869–1875.
[98] C. Hock, K. Villringer, F. Müller-Spahn, et al., Decrease in parietal cerebral hemoglobin oxygenation during performance of a verbal fluency task in patients with Alzheimer's disease monitored by means of near-infrared spectroscopy (NIRS) — correlation with simultaneous rCBF-PET measurements, Brain Res. 755 (1997) 293–303.
[99] C.F. Lourenço, A. Ledo, R.M. Barbosa, et al., Neurovascular uncoupling in the triple transgenic model of Alzheimer's disease: impaired cerebral blood flow response to neuronal-derived nitric oxide signaling, Exp. Neurol. 291 (2017) 36–43.
[100] K. Kotliar, C. Hauser, M. Ortner, et al., Altered neurovascular coupling as measured by optical imaging: a biomarker for Alzheimer's disease, Sci. Rep. 7 (2017) 1–11.
[101] N. Cholet, J. Seylaz, P. Lacombe, et al., Local uncoupling of the cerebrovascular and metabolic responses to somatosensory stimulation after neuronal nitric oxide synthase inhibition, J. Cereb. Blood Flow Metab. 17 (1997) 1191–1201.
[102] J. Gotoh, T.-Y. Kuang, Y. Nakao, et al., Regional differences in mechanisms of cerebral circulatory response to neuronal activation, Am. J. Physiol. Heart Circ. Physiol. 280 (2001) H821–H829.
[103] C. Ayata, J. Ma, W. Meng, et al., L-NA-sensitive rCBF augmentation during vibrissal stimulation in type III nitric oxide synthase mutant mice, J. Cereb. Blood Flow Metab. 16 (1996) 539–541.
[104] C. Aoki, D.S. Bredt, S. Fenstemaker, et al., The subcellular distribution of nitric oxide synthase relative to the NRl subunit of NMDA receptors in the cerebral cortex, Prog. Brain Res. 118 (1998) 83–97.
[105] D. Standaert, NMDA receptors and nitric oxide synthase, Mol. Psychiatr. 4 (1999) 13–14.
[106] N. Hardingham, J. Dachtler, K. Fox, The role of nitric oxide in pre-synaptic plasticity and homeostasis, Front. Cell. Neurosci. 7 (2013) 1–19.
[107] U. Forstermann, E.I. Closs, J.S. Pollock, et al., Nitric oxide synthase isozymes characterization, purification, molecular cloning, and functions, Hypertension 23 (1994) 1121–1131.
[108] T. David, K. Dormanns, R.G. Brown, The role of nitric oxide in neurovascular coupling, J. Theor. Biol. 394 (2014) 1–17.
[109] W. Meng, C. Ayata, C. Waeber, et al., Neuronal NOS-cGMP-dependent ACh-induced relaxation in pial arterioles of endothelial NOS knockout mice, Am. J. Physiol. 274 (1998) 411–415.
[110] D. Sun, H. Liu, C. Yan, et al., COX-2 contributes to the maintenance of flow-induced dilation in arterioles of eNOS-knockout mice, Am. J. Physiol. Heart Circ. Physiol. 291 (2006) H1429–H1435.
[111] H. Hara, C. Waeber, P.L. Huang, et al., Brain distribution of nitric oxide synthase in neuronal or endothelial nitric oxide synthase mutant mice using [3H]L-NG-Nitro-Arginine autoradiography, Neuroscience 75 (1996) 881–890.
[112] H. Son, R.D. Hawkins, K. Martin, Long-term potentiation is reduced in mice that are doubly mutant in endothelial and neuronal nitric oxide synthase, Cell 87

(1996) 1015–1023.
[113] J. Zhang, S.H. Snyder, Nitric oxide in the nervous system, Annu. Rev. Pharmacol. Toxicol. 35 (1995) 213–233.
[114] M. Endoh, K. Maiese, J.A. Wagner, Expression of the neural form of nitric oxide synthase by CA1 hippocampal neurons and other central nervous system neurons, Neuroscience 63 (1994) 679–689.
[115] D.L. Drazen, S.L. Klein, A.L. Burnett, et al., Reproductive function in female mice lacking the gene for endothelial nitric oxide synthase, Nitric Oxide 3 (1999) 366–374.
[116] A. Jablonka-Shariff, S. Ravi, A.N. Beltsos, et al., Abnormal estrous cyclicity after disruption of endothelial and inducible nitric oxide synthase in mice, Biol. Reprod. 61 (1999) 171–177.
[117] L.K. Bak, A. Schousboe, H.S. Waagepetersen, The glutamate/GABA-glutamine cycle: aspects of transport, neurotransmitter homeostasis and ammonia transfer, J. Neurochem. 98 (2006) 641–653.
[118] Y. Daikhin, M. Yudkoff, Compartmentation of brain glutamate metabolism in neurons and glia, J. Nutr. 130 (2000) 1026S–1031S.
[119] J. Albrecht, M. Sidoryk-Węgrzynowicz, M. Zielińska, et al., Roles of glutamine in neurotransmission, Neuron Glia Biol. 6 (2004) 263–276.
[120] S.R. Jaffrey, H. Erdjument-Bromage, C.D. Ferris, et al., Protein S-nitrosylation: a physiological signal for neuronal nitric oxide, Nat. Cell Biol. 3 (2001) 193–197.
[121] E. Kosenko, M. Llansola, C. Montoliu, Glutamine synthetase activity and glutamine content in brain: modulation by NMDA receptors and nitric oxide, Neurochem. Int. 43 (2003) 493–499.
[122] W.C. Sessa, M. Hecker, J.A. Mitchell, et al., The metabolism of L-arginine and its significance for the biosynthesis of endothelium-derived relaxing factor: L-Glutamine inhibits the generation of L-arginine by cultured endothelial cells, Proc. Natl. Acad. Sci. Unit. States Am. 87 (1990) 8607–8611.
[123] G.L. Prince, P. Delaere, C. Fages, et al., Glutamine synthetase (GS) expression is reduced in senile dementia of the Alzheimer type, Neurochem. Res. 20 (1995) 859–862.
[124] M. Fisman, M. Ball, W. Blume, Hyperammonemia in Alzheimer's disease, Am. J. Psychiatry 142 (1985) 71–73.
[125] S. Hoyer, R. Nitsch, K. Oesterreich, Ammonia is endogenously generated in the brain in the presence of presumed and verified dementia of Alzheimer type, Neurosci. Lett. 117 (1990) 358–362.
[126] R. Branconnier, E. Dessain, M. McNiff, et al., Blood ammonia and Alzheimer's disease, Am. J. Psychiatry 143 (1986) 1313–1314.
[127] S.M. Morris Jr., Regulation of enzymes of the urea cycle and arginine metabolism, Annu. Rev. Nutr. 22 (2002) 87–105.
[128] F. Bensemain, D. Hot, S. Ferreira, et al., Evidence for induction of the ornithine transcarbamylase expression in Alzheimer's disease, Mol. Psychiatr. 14 (2009) 106–116.
[129] D.R. Demady, S. Jianmongkol, J.L. Vuletich, et al., Agmatine enhances the NADPH oxidase activity of neuronal NO synthase and leads to inactivation of the enzyme, Mol. Pharmacol. 59 (2001) 24–29.
[130] S. Regunathan, J.E. Piletz, Regulation of inducible nitric oxide synthase and agmatine synthesis in macrophages and astrocytes, Ann. N. Y. Acad. Sci. 1009 (2003) 20–29.
[131] C.H. Mun, W.T. Lee, K.A. Park, et al., Regulation of endothelial nitric oxide synthase by agmatine after transient global cerebral ischemia in rat brain, Anat Cell Biol 43 (2010) 230–240.
[132] D.H. Bergin, Y. Jing, H. Zhang, et al., A single intracerebroventricular AB25–35 infusion leads to prolonged alterations in arginine metabolism in the rat hippocampus and prefrontal cortex, Neuroscience 298 (2015) 367–379.